Structurally Unusual Trihydrido–Triosmium Clusters

Shariff E. Kabir and Edward Rosenberg*

Department of Chemistry, The University of Montana, Missoula, Montana 59812

M. Day and Kenneth I. Hardcastle

Department of Chemistry, California State University, Northridge, Northridge, California 91330

Received June 2, 1994[⊗]

The reactions of $(\mu\text{-H})(\mu_3\text{-}\eta^2\text{-}\overline{\text{C=NCH}_2\text{CH}_2\text{CH}_2}\text{)Os}_3(\text{CO})_9$ (**1**) with H_2, H_2S, and C_2H_5SH are reported. In the case of H_2 a trihydrido cluster in which all metal–metal bonds are retained is formed, $H(\mu\text{-H})_2(\mu_3\text{-}\eta^2\text{-}\overline{\text{C=NCH}_2\text{CH}_2\text{CH}_2}\text{)Os}_3(\text{CO})_8$ (**2**), along with minor byproducts. The hydrides in **2** are rigid on the NMR time scale, but reaction with PPh_3 yields the related $H(\mu\text{-H})_2(\mu\text{-}\eta^2\text{-}\overline{\text{C=dbdNCH}_2\text{CH}_2\text{CH}_2}\text{)Os}_3(\text{CO})_8\text{PPh}_3$ (**5**), in which the hydrides exhibit dynamic behavior on the NMR time scale which has been examined in detail. The reaction of **1** with H_2S yields a set of isomeric trihydride clusters in which two of the three metal–metal bonds have been cleaved, $H_2(\mu\text{-H})(\mu_3\text{-S})(\mu\text{-}\eta^2\text{-}\overline{\text{C=NCH}_2\text{CH}_2\text{CH}_2}\text{)Os}_3(\text{CO})_9$ (**7**), while reaction with C_2H_5SH yields the dihydride $H(\mu\text{-H})(\mu\text{-S})(\mu\text{-}\eta^2\text{-}\overline{\text{C=NCH}_2\text{CH}_2\text{CH}_2}\text{)Os}_3(\text{CO})_9$ (**8**), whose structure and isomers help elucidate the pathway of formation of **7**. Solid-structures of **2**, **5**, and **7a** are reported. Compound **2** crystallizes in the monoclinic space group $P2_1/n$ with unit cell parameters $a = 7.113(2)$ Å, $b = 16.227(2)$ Å, $c = 15.171(3)$ Å, $\beta = 91.33(2)°$, $V = 1751(1)$ Å^3, and $Z = 4$. Least-squares refinement of 1837 observed reflections gave a final agreement factor of $R = 0.054$ ($R_w = 0.061$). Compound **5** crystallizes in space group *Pbca* with unit cell parameters $a = 15.230(3)$ Å, $b = 16.871(2)$ Å, $c = 24.947(5)$ Å, $V = 6410(3)$ Å^3, and $Z = 8$. Least-squares refinement of 3943 observed reflections gave a final agreement factor of $R = 0.050$ ($R_w = 0.053$). Compound **7a** crystallizes in the monoclinic space group $P2_1/n$ with unit cell parameters $a = 10.541(2)$ Å, $b = 15.151(3)$ Å, $c = 12.281(3)$ Å, $\beta = 91.35(2)°$, $V = 1961(1)$ Å^3, and $Z = 4$. Least-squares refinement of 2408 observed reflections gave a final agreement factor of $R = 0.058$ ($R_w = 0.067$).

Introduction

There are numerous examples in the literature of polyhydrido–trimetallic clusters.[1] In this class of compounds, the hydride ligands almost invariably adapt the edge-bridging bonding mode, with the notable exceptions being $H(\mu\text{-H})Os_3(CO)_{10}L$ (L = 2e donor), which contains a terminal and a bridging hydride that undergo site exchange on the NMR time scale,[2–4] and $H(\mu\text{-H})_3Os_3(\mu_3\text{-}\eta^1\text{-NCH}_2CF_3)(CO)_8$, containing one terminal and three bridging hydrides which are rigid on the NMR time scale.[11] In the case of trihydride species, the most common structural type has one edge-bridging hydride on each edge of the metal triangle, and investigations of the ligand dynamics in these systems have shown that the hydrides are invariably rigid even at elevated temperatures.[5] During the course of our studies on the general reactivity of μ_3-imidoyl trimetallic clusters we synthesized a structurally unusual trihydride complex containing two bridging hydrides and one terminal metal hydride by reaction with dihydrogen. These hydrides are initially stereochemically rigid but become dynamic on the NMR time scale upon coordination of an additional ligand. In a related study the reaction of a μ_3-imidoyl cluster with H_2S gives a trimetallic species containing two terminal and one bridging hydride. We report here the details of the structures and the ligand dynamics of these structurally unusual trihydride clusters.

Results and Discussion

Dihydrogen has been shown to react with a variety of osmium clusters. The reaction of H_2 with $Os_3(CO)_{12}$

[⊗] Abstract published in *Advance ACS Abstracts,* October 1, 1994.

(1) (a) Lavigne, G. In *The Chemistry of Metal Cluster Complexes*; Shriver, D. F., Kaesz, H. D., Adams, R. D., Eds.; VCH: New York, 1990. (b) Deeming, A. J. *Adv. Organomet. Chem.* **1983**, *26*, 1. (c) Bower, D. K.; Keister, J. B. *Organometallics* **1990**, *9*, 2321. (d) Calvert, R. B.; Shapley, J. R. *J. Am. Chem. Soc.* **1977**, *99*, 5225. (e) Azam, K. A.; Deeming, A. J.; Rothwell, I. P. *J. Chem. Soc., Dalton Trans.* **1981**, 91. (f) Deeming, A. J.; Underhill, M. *J. Chem. Soc., Chem. Commun.* **1973**, 277. (g) Shore, S. G.; Jan, D.-Y.; Hsu, L.-Y.; Hsu, L.-W.; Kennedy, S.; Huffman, J. C.; Lin Wang, T.-C.; Marshall, A. G. *J. Chem. Soc., Chem. Commun.* **1984**, 392. (h) Keister, J. B.; Horling, T. L. *Inorg. Chem.* **1980**, *19*, 2304. (i) Keister, J. B. *J. Chem. Soc., Chem. Commun.* **1979**, 214. (j) Keister, J. B.; Payne, M. W.; Muscatella, M. J. *Organometallics* **1983**, *2*, 219. (k) Shapley, J. R.; Strickland, D. S.; St. George, G. M.; Churchill, M. R.; Bueno, D. *Organometallics* **1983**, *2*, 185. (l) Mays, M. L.; Dawoodi, Z.; Henrick, K. *J. Chem. Soc., Dalton Trans.* **1984**, 433.

(2) (a) Aime, S.; Osella, D.; Milone, L.; Rosenberg, E. *J. Organomet. Chem.* **1981**, *213*, 207. (b) Rosenberg, E.; Anslyn, E. V.; Barner-Thorsen, C.; Aime, S.; Osella, D.; Gobetto, R.; Milone, L. *Organometallics* **1984**, 1790.

(3) Adams, R. D.; Golembeski, N. M. *Inorg. Chem.* **1979**, *18*, 1909.

(4) Keister, J. B.; Shapley, J. R. *Inorg. Chem.* **1982**, *21*, 3304.

(5) Nevinger, L. R.; Keister, J. B. *Organometallics* **1990**, *9*, 2312 and references therein.

0276-7333/94/2313-4437$04.50/0

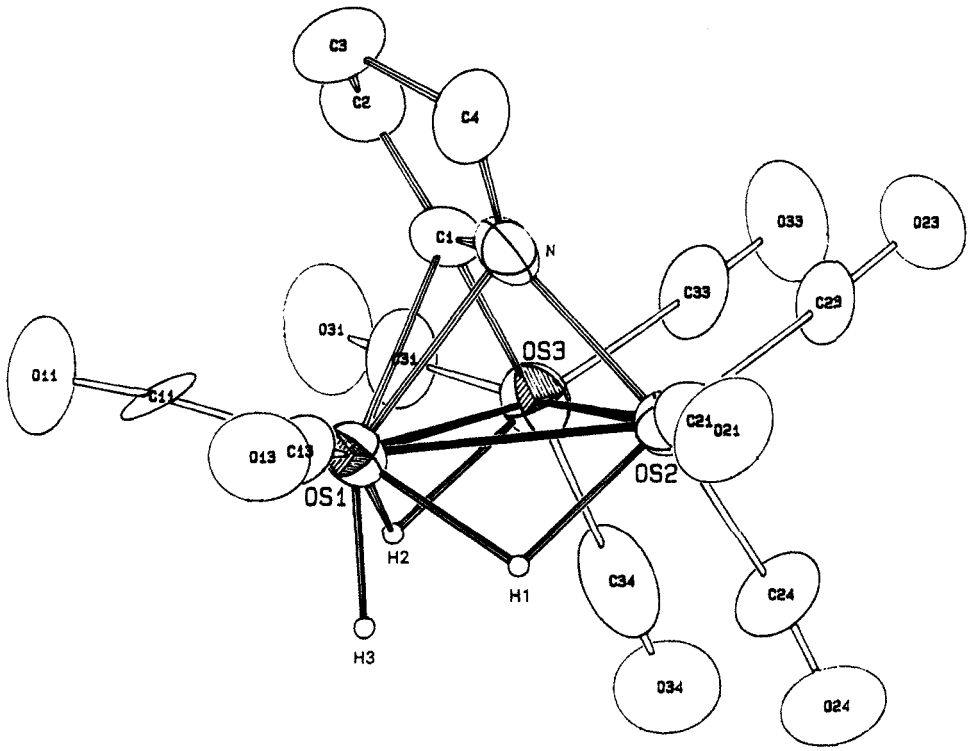

Figure 1. ORTEP drawing of $H(\mu\text{-}H)_2(\mu_3\text{-}\eta^2\text{-}\overline{C{=}NCH_2CH_2CH_2})Os_3(CO)_8$ (**2**) showing the calculated positions of the hydrides.

gives $(\mu\text{-}H)_2Os_3(CO)_{10}$,[6] that with $(\mu_3\text{-}\eta^2\text{-}(C_6H_5)C{=}C(C_6H_5))Os_3(CO)_{10}$ gives $(\mu\text{-}H)_2(\mu_3\text{-}\eta^2\text{-}(C_6H_5)C{=}C(C_6H_5))Os_3(CO)_9$,[7] that with $(\mu\text{-}(C_6H_5)_2PCH_2P(C_6H_5)_2))Os_3(CO)_{10}$ gives $(\mu\text{-}H)_2(\mu\text{-}C_6H_5)_2PCH_2P(C_6H_5)_2)Os_3(CO)_8$,[8] and that with $(\mu\text{-}H)(\mu\text{-}C_6H_5)_2PCH_2P(C_6H_5)(C_6H_4))Os_3(CO)_9$ gives $(\mu\text{-}H)_2(\mu\text{-}C_6H_5)_2PCH_2P(C_6H_5)_2)Os_3(CO)_8$.[9] In three of the above examples the hydrogen has added to the cluster as a bridging hydride, while in one the organic ligand has been hydrogenated as well. We decided to react $(\mu\text{-}H)(\mu_3\text{-}\eta^2\text{-}\overline{C{=}NCH_2CH_2CH_2})Os_3(CO)_9$ (**1**) with dihydrogen in order to ascertain which of the above processes would occur in the case of imidoyl complexes.

The reaction of **1** with 1 atm of dihydrogen in refluxing octane gives one major product, whose infrared and ^1H NMR spectra and elemental analysis indicated the molecular formula $H(\mu\text{-}H)_2(\mu_3\text{-}\eta^2\text{-}\overline{C{=}NCH_2CH_2CH_2})Os_3(CO)_8$ (**2**; eq 1) in 46% yield based on consumed **1**. In

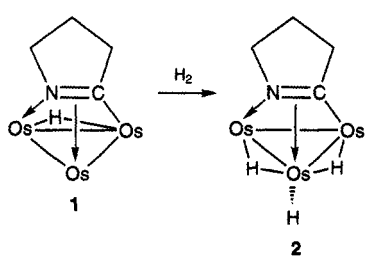

1 2 (1)

addition, two minor products were obtained which were identifed as $(\mu\text{-}H)(\mu\text{-}\eta^2\text{-}\overline{C{=}NCH_2CH_2CH_2})Os_3(CO)_{10}$[10] (**3**) and $(\mu\text{-}H)_2(\mu\text{-}\eta^2\text{-}\overline{C{=}NCH_2CH_2CH_2})_2Os_3(CO)_8$[11] (**4**) on the basis of their infrared and ^1H NMR spectra. Compound **2** is also obtained in similar yield (47%) by photolysis of **1** in the presence of 1 atm of dihydrogen in hexane for 1 h. The formation of **3** and **4** was not observed under these conditions, but one additional unidentified product was obtained in trace amounts. Irradiation of **1** under these conditions for longer periods of time resulted only in decomposition of **1** and **2**.

It was apparent from the ^1H NMR data that **2** contained one terminal (−9.65 ppm) and two bridging (−15.31 and −15.89 ppm) hydrides, but because of the low symmetry of this cluster, we could not definitively assign the structure shown (eq 1). We therefore undertook a solid-state structural investigation of **2**. The solid-state structure of **2** is shown in Figure 1. Crystal data are given in Table 1, and selected bond distances and angles are given in Table 2 and atomic coordinates in Table 3. Compound **2** exists as a triangular core of osmium atoms with three nearly equivalent metal−metal bonds (Os(1)−Os(2) = 2.836(1) Å, Os(1)−Os(3) = 2.857(2) Å, and Os(2)−Os(3) = 2.817(1) Å). The organic ligand serves as a five-electron donor by donating one electron through a σ-bond from C(1) to Os(3) (C(1)−Os(3) = 2.10(3) Å), two electrons by a donor σ-bond between N and Os(2) N−Os(2) = 2.11(2) Å), and two additional electrons *via* a π-bond from the double bond between C(1) and N (C(1)−N = 1.39(3) Å) and Os(1)

(6) Knox, S. A. R.; Koepke, J. W.; Andrews, M. A.; Kaesz, H. D. *J. Am. Chem. Soc.* **1975**, *97*, 3942.
(7) (a) Tachikawa, M.; Shapley, J. R.; Pierpont, C. G. *J. Am. Chem. Soc.* **1975**, *16*, 7172. (b) Pierpont, C. G. *Inorg. Chem.* **1977**, *16*, 636.
(8) Deeming, A. J.; Kabir, S. E. *J. Organomet. Chem.* **1988**, 340−359.
(9) Clucas, J. A.; Harding, M. M.; Smith, A. K. *J. Chem. Soc., Chem. Commun.* **1985**, 1280.
(10) (a) Day, M.; Espitia, D.; Hardcastle, K. I.; Kabir, S. E.; McPhillips, T.; Rosenberg, E.; Gobetto, R.; Milone, L.; Osella, D. *Organometallics* **1993**, *12*, 2309. (b) Rosenberg, E.; Kabir, S. E.; Hardcastle, K. I.; Day, M.; Wolf, E. *Organometallics* **1990**, *9*, 2214. (c) Rosenberg, E.; Freeman, W.; Carlos, Z.; Hardcastle, K.; Yoo, Y. J.; Milone, L.; Gobetto, R. *J. Cluster Sci.* **1992**, *3*, 439.
(11) Rosenberg, E.; Kabir, S. E.; Day, M.; Hardcastle, K. I.; McPhillips, T.; Wolf, E. *Organometallics*, submitted for publication.

Table 1. Crystallographic Data Collection and Refinement Parameters for 2, 5, and 7a

	2	5	7a
formula	$C_{12}H_9Os_3NO_8$	$C_{30}H_{24}Os_3NO_8P$	$C_{13}H_9Os_3NO_9S$
fw	865.81	1128.10	925.88
cryst dimens, mm³	0.40 × 0.40 × 0.06	0.09 × 0.08 × 0.32	0.08 × 0.25 × 0.30
radiation; wavelength, Å	Mo; 0.709 30	Mo; 0.710 73	Mo; 0.709 30
temp, °C	25 ± 1	25 ± 1	25 ± 1
cryst syst	monoclinic	orthorhombic	monoclinic
space group	$P2_1/n$	*Pbca*	$P2_1/n$
a, Å	7.113(2)	15.230(3)	10.541(2)
b, Å	16.227(2)	16.871(2)	15.151(3)
c, Å	15.171(3)	24.947(5)	12.281(3)
β, deg	91.33(2)		91.35(2)
V, Å³	1751(1)	6410(3)	1961(1)
Z	4	8	4
density, g/cm³	3.29	2.34	3.14
abs coeff, μ, cm^{-1}	217.9	119.8	195.7
rel transmissn coeff	0.142–0.999		0.189–0.996
scan type	ω–2θ	ω–2θ	ω–2θ
scan rate, deg/min	4.50–8.23	1.20–5.49	6.75–8.23
scan width, deg	1.0 + 0.350 tan θ	0.8 + 0.350 tan θ	0.8 + 0.350 tan θ
hkl ranges	*h*, −7 to +7; *k*, 0–17; *l*, 0–16	*h*, 0–20; *k*, 0–16; *l*, 0–32	*h*, −12 to +12; *k*, −17 to +17; *l*, 0–14
2θ range, deg	4.0–46.0	4.0–56.0	4.0–50.0
structure soln	Patterson method	Patterson method	Patterson method
no. of unique data	2543	7515	3597
no. of data used in LS refinement with $F_o > 3.0\sigma(F_o)$	1837	3942	2408
weighting scheme, *w*	$4F_o^2/[\sigma(F_o)^2]^2$	$4F_o^2/[\sigma(F_o)^2]^2$	$4F_o^2/[\sigma(F_o)^2]^2$
no. of params refined	217	388	241
R^a	0.0536	0.0500	0.0585
$R_w{}^b$	0.0613	0.0529	0.0618
esd of observn of unit weight (GOF)	2.09	1.30	1.57
largest shift/esd	0.01	0.01	0.06
highest peak in final diff map, e/Å³	1.53 (52)	1.34 (30)	1.86 (48)

[a] $R = \sum[|F_o| - |F_c|]\sum |F_o|$. [b] $R_w = [\sum w(|F_o| - |F_c|)^2/\sum w|F_o|^2]^{1/2}$.

Table 2. Selected Bond Distances (Å) and Angles (deg) for 2[a]

	Distances		
Os(1)–Os(2)	2.836(1)	C(1)–N	1.39(3)
Os(1)–Os(3)	2.857(2)	C(1)–C2	1.44(4)
Os(2)–Os(3)	2.817(1)	C(2)–C3	1.59(4)
		C(3)–C4	1.55(3)
Os(1)–N	2.29(2)	C(4)–N	1.50(3)
Os(1)–C(1)	2.35(2)		
Os(2)–N	2.11(2)		
Os(3)–C(1)	2.10(3)	Os(1)–H(3)	1.60[c]
		Os(1)–H(2)	1.85[c]
		Os(1)–H(1)	1.81[c]
Os–C(CO)	1.89(3)[b]		
C–O	1.14(3)[b]		
	Angles		
Os(1)–Os(2)–Os(3)	60.73(3)	Os–C–O	175.6(3)[b]
Os(2)–Os(3)–Os(1)	59.97(3)		
Os(2)–Os(1)–Os(3)	59.30(3)	H(1)–Os(1)–H(2)	82[c]
N–Os(2)–Os(1)	52.8(5)	H(1)–Os(1)–H(3)	59[c]
C(1)–Os(3)–Os(1)	54.0(5)	H(2)–Os(1)–H(3)	53[c]

[a] Numbers in parenthesis are estimated standard deviations. [b] Average values. [c] Values calculated using HYDEX.[12]

(N–Os(1) = 2.29(2) Å and C(1)–Os(1) = 2.35(2) Å). All but the last two metal–ligand bond lengths are very similar to those in **1**.[10b] The positions of the hydrides were calculated using the program HYDEX,[12] where the program was allowed to search for potential energy minima along all three metal edges for bridging hydrides and all three osmium atoms for terminal hydrides. Two bridging hydrides and one terminal hydride position were found. The bridging hydrides were found along the edges of the cluster not bridged by the organic ligand, tucked down below the plane of the metals (1.09 Å for H(1) and 0.95 Å for H(2)). Their positions as *trans* to CO(11) and CO(23) for H(1) and *trans* to CO(33) and CO(13) for H(2) verify these calculated positions.[10] The terminal hydride was found to be bonded to the rear metal atom, Os(1), where a CO ligand is located in the parent compound **1**.[10a]

(12) Orpen, A. G. *J. Chem. Soc., Dalton Trans.* **1980**, 2509.

Table 3. Fractional Atomic Coordinates for 2

atom	*x*	*y*	*z*	*B* (Å²)[a]
Os(1)	−0.3628(1)	−0.19042(7)	0.13049(6)	2.92(2)
Os(2)	−0.1435(1)	−0.28195(7)	0.25450(5)	2.98(2)
Os(3)	−0.1636(1)	−0.33440(7)	0.07755(6)	3.38(2)
O(11)	−0.454(3)	−0.094(1)	−0.035(1)	5.9(5)
O(13)	−0.460(3)	−0.042(1)	0.236(1)	5.7(5)
O(21)	−0.153(3)	−0.182(1)	0.424(1)	5.7(5)
O(23)	0.243(3)	−0.356(2)	0.287(1)	6.8(6)
O(24)	−0.345(3)	−0.429(1)	0.328(1)	6.0(5)
O(31)	−0.179(3)	−0.339(1)	−0.125(1)	7.1(6)
O(33)	0.204(3)	−0.427(2)	0.092(1)	8.1(6)
O(34)	−0.385(3)	−0.491(1)	0.114(1)	7.0(6)
N	−0.050(2)	−0.187(1)	0.171(1)	3.4(4)
C(1)	−0.054(3)	−0.214(2)	0.085(1)	3.2(5)
C(2)	0.046(3)	−0.159(2)	0.028(1)	4.3(7)
C(3)	0.073(4)	−0.077(2)	0.086(1)	3.9(6)
C(4)	0.064(4)	−0.110(2)	0.182(1)	4.4(6)
C(11)	−0.412(3)	−0.127(2)	0.027(1)	4.0(5)
C(13)	−0.417(3)	−0.100(2)	0.194(1)	3.6(6)
C(21)	−0.148(3)	−0.215(2)	0.359(1)	4.3(7)
C(23)	0.092(3)	−0.329(2)	0.275(2)	3.7(6)
C(24)	−0.259(4)	−0.375(2)	0.302(2)	4.1(6)
C(31)	−0.179(4)	−0.337(2)	−0.050(2)	4.8(7)
C(33)	0.062(4)	−0.392(2)	0.089(2)	4.5(6)
C(34)	−0.302(4)	−0.434(2)	0.098(2)	5.2(6)
H(1)	−0.392	−0.254	0.230	4.0*
H(2)	−0.404	−0.290	0.074	4.0*
H(3)	−0.543	−0.249	0.140	4.0*

[a] Starred values denote atoms given fixed *B*'s. Anisotropically refined atoms are given in the form of the isotropic equivalent displacement parameter, defined as $^4/_3[a^2B_{11} + b^2B_{22} + c^2B_{33} + ab(\cos\gamma)B_{12} + ac(\cos\beta)B_{13} + bc(\cos\alpha)B_{23}]$.

Although the hydrides in **2** are cleary rigid on the NMR time scale with respect to the bridge–terminal exchange, the chiral nature of the cluster makes the carbonyl groups on Os(1) diastereotopic. It is therefore possible that the $(CO)_2H$ grouping on Os(1) is undergoing tripodal motion. The proton-decoupled ^{13}C NMR spectrum of **2** at room temperature shows the expected eight resonances. The observation of two complex multiplets for two carbonyls allows partial assignment of these resonances to the radial carbonyl groups on Os(1) and confirms that these ligands are rigid on the NMR time scale. The rigidity of the ligands on Os(1) in **2** is in sharp contrast to those for the three carbonyl groups on the analogous osmium atom in **1**, which are undergoing tripodal motion on the NMR time scale even at −60 °C, where the "windshield wiper" of the hydride and the imidoyl ligand is slow on the NMR time scale.[10] This difference is attributable to the presence of the bridging hydrides or the different bonding properties of the terminal hydride in **2**.

Since the stereochemically nonrigid **1** undergoes facile reactions with two-electron donors with apparent displacement of the C=N π-bond,[10,13] we thought it would be interesting to see if the stereochemically rigid **2** would exhibit the same type of reactivity. Indeed, treatment of **2** with triphenylphosphine at ambient temperatures for 24 h leads to conversion to a single product in 86% isolated yield whose ^1H and ^{31}P NMR and infrared spectra and elemental analysis are consistent with the formula $H(\mu\text{-}H)_2(\mu\text{-}\eta^2\text{-}\overline{C{=}NCH_2\text{-}CH_2CH_2})Os_3(CO)_8PPh_3$ (**5**), where the phosphine has coordinated to the osmium atom formerly π-bonded to the C=N bond (eq 2).

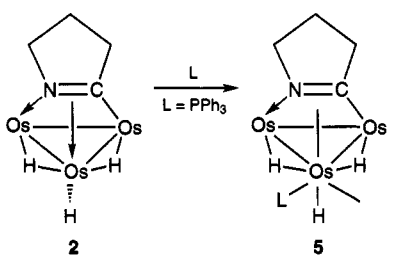

2 **5** (2)

Here again as for **2**, although it was clear what the approximate structure of **5** was (eq 2), the exact disposition of hydride ligands was unclear, and so a solid-state structure determination of **5** was undertaken. The solid-state structure of **5** is shown in Figure 2; selected distances and bond angles are given in Table 4, atomic coordinates in Table 5, and crystal data in Table 1. Although the connectivity of the hydrides in **5** is similar to that in **2**, phosphine addition results in significant changes in several aspects of the structure. Both metal–metal bonds bearing the bridging hydrides are elongated by ~0.2 Å relative to **2**, and this is accompanied by a dramatic change in location of the bridging hydrides, which HYDEX finds on the same face of the Os_3 triangle as the imidoyl ligand. This location is again supported by the disposition of the phosphine and CO(21) with one distinctly tilted toward the opposite face. The overall geometry at Os(2), the metal atom bonded to all three hydrides, is octahedral (excluding the metal–metal vectors), and the $Os(2)P(CO)_2H_3$ moiety tilts away from the μ-imidoyl on the Os(1)–Os(3) edge. Thus, the terminal hydrides make an angle of 77° with the metal triangle, while the corresponding angle in **2** is 93°. Similarly, CO(22) makes a distinctly obtuse angle with the metal triangle, while in **3** the related carbonyl is perpendicular to the osmium core.[10b] In both **5** and **3** the μ-bonded imidoyl is essentially perpendicular to the osmium triangle. All of these structural comparisons can be rationalized on the basis of the relative steric requirements of the CO, H, and PPh_3 ligands.

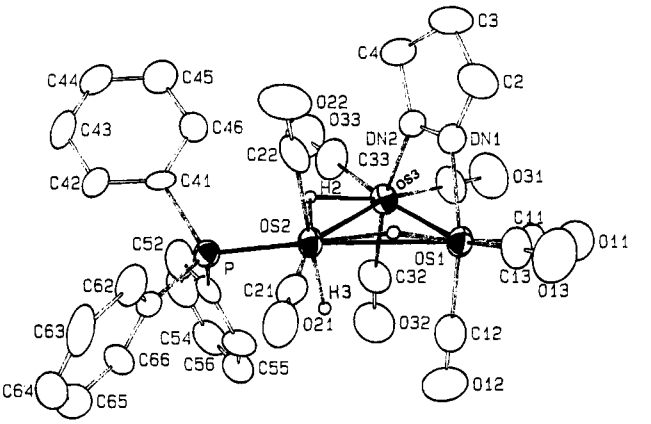

Figure 2. ORTEP drawing of $H(\mu\text{-}H)_2(\mu\text{-}\eta^2\overline{HC{=}NCH_2\text{-}CH_2CH_2})Os_3(CO)_8PPh_3$ (**5**) showing the calculated positions of the hydrides.

Table 4. Selected Bond Distances (Å) and Angles (deg) for 5[a]

	Distances		
Os(1)–Os(2)	3.0663(8)	DN1–DN2[b]	1.28(2)
Os(1)–Os(3)	2.7937(9)	DN1–C(2)[b]	1.49(2)
Os(2)–Os(3)	3.0891(8)	DN2–C(4)[b]	1.54(2)
		C(2)–C(3)	1.58(2)
Os(1)–DN1[b]	2.10(1)	C(3)–C(4)	1.58(2)
Os(3)–DN2[b]	2.08(1)		
Os(2)–P	2.332(4)	Os(2)–H(1)	1.85[d]
Os–C(CO)	1.90(2)[c]	Os(2)–H(2)	1.85[d]
C–O	1.14(2)	Os(2)–H(3)	1.60[d]
	Angles		
Os(1)–Os(2)–Os(3)	53.98(2)	DN2–Os(3)–Os(2)	83.0(3)
Os(1)–Os(3)–Os(2)	62.59(2)	H(1)–Os(2)–H(2)	111[d]
Os(2)–Os(1)–Os(3)	63.43(2)	H(1)–Os(2)–H(3)	99[d]
Os–C–O	177(2)[c]	H(2)–Os(2)–H(3)	91[d]
DN1–Os(1)–Os(2)	85.5(4)		

[a] Numbers in parentheses are estimated standard deviations. [b] DN1 and DN2 designate an average of carbon and nitrogen nucleii (6.5 protons) used in the refinement to compensate for the disordering of these atoms in the structure. [c] Average values. [d] Values calculated using HYDEX.[12]

We have been able to measure an approximate rate for the formation of **5** by following the disappearance of **2** by ^1H NMR in the hydride region. It was not possible to monitor the rate of appearance of **5**, since its hydride resonances are broadened by exchange and because it exists as several isomers in solution (*vide infra*). Using the rate of decay of the resonances of **2**, we can estimate a second-order rate constant of 2.0 ± 1.2 M^{-1} min^{-1}, over 100 times faster than the rate constant for triphenylphosphine addition of **1** (0.012 ± 0.004 M^{-1} min^{-1}).[10c] This result clearly indicates that the relatively high reactivity of complexes such as **1** is due to the facile displacement of the C=N π-bond from the metal it is coordinated to rather than partial opening of a coordi-

(13) Day, M.; Espitia, D.; Hardcastle, K. I.; Kabir, S. E.; Rosenberg, E.; Gobetto, R.; Milone, L.; Osella, D. *Organometallics* **1991**, *10*, 3550.

Table 5. Fractional Atomic Coordinates for 5

atom	*x*	*y*	*z*	*B* (Å^2)[a]
Os(1)	0.15898(4)	0.09862(4)	0.03521(2)	3.28(1)
Os(2)	0.34356(4)	0.08796(3)	0.08377(2)	2.85(1)
Os(3)	0.19608(4)	0.20180(4)	0.11982(2)	3.30(1)
P	0.4435(2)	0.0935(2)	0.1545(1)	2.93(7)
O(11)	−0.0348(8)	0.1397(9)	0.0353(6)	8.9(4)
O(12)	0.1160(9)	−0.0458(8)	0.1030(5)	7.0(3)
O(13)	0.1406(9)	0.0211(8)	−0.0736(5)	7.7(4)
O(21)	0.4253(7)	−0.0571(7)	0.0328(5)	5.8(3)
O(22)	0.4457(9)	0.2009(8)	0.0111(5)	7.2(3)
O(31)	0.0144(8)	0.2751(9)	0.1152(6)	8.4(4)
O(32)	0.1343(9)	0.0824(8)	0.2020(5)	7.1(4)
O(33)	0.264(1)	0.3303(8)	0.1936(5)	8.0(4)
DN1	0.1990(8)	0.2103(8)	0.0066(5)	3.5(3)
DN2	0.2207(8)	0.2547(7)	0.0460(5)	3.0(3)
C(2)	0.214(1)	0.245(1)	−0.0477(5)	5.3(4)
C(3)	0.239(1)	0.334(1)	−0.0346(6)	5.5(4)
C(4)	0.260(1)	0.3340(9)	0.0275(6)	4.4(4)
C(11)	0.040(1)	0.125(1)	0.0366(7)	5.1(4)
C(12)	0.133(1)	0.006(1)	0.0768(6)	4.8(4)
C(13)	0.150(1)	0.052(1)	−0.0339(6)	4.5(4)
C(21)	0.395(1)	−0.0005(9)	0.0524(6)	4.1(4)
C(22)	0.4074(9)	0.161(1)	0.0389(6)	4.0(3)
C(31)	0.082(1)	0.247(1)	0.1173(6)	5.1(4)
C(32)	0.161(1)	0.129(1)	0.1725(6)	4.6(4)
C(33)	0.242(1)	0.282(1)	0.1660(5)	5.5(4)
C(41)	0.5150(9)	0.1811(7)	0.1589(5)	2.7(3)
C(42)	0.0561(9)	0.1747(9)	0.1816(6)	3.5(3)
C(43)	0.6452(9)	0.245(1)	0.1915(6)	4.8(4)
C(44)	0.611(1)	0.3175(9)	0.1793(7)	5.0(4)
C(45)	0.530(1)	0.324(1)	0.1546(8)	5.4(4)
C(46)	0.481(1)	0.256(1)	0.1448(6)	4.4(4)
C(51)	0.3929(9)	0.0911(9)	0.2209(5)	3.5(3)
C(52)	0.415(1)	0.151(1)	0.2593(6)	5.0(4)
C(53)	0.375(1)	0.145(1)	0.3105(7)	6.3(5)
C(54)	0.316(1)	0.086(1)	0.3210(6)	5.8(4)
C(55)	0.295(1)	0.028(1)	0.2833(6)	5.1(4)
C(56)	0.332(1)	0.033(1)	0.2317(6)	4.6(4)
C(61)	0.5211(9)	0.0122(7)	0.1557(5)	3.0(3)
C(62)	0.5745(9)	0.001(1)	0.1092(6)	4.3(4)
C(63)	0.6341(9)	−0.064(1)	0.1102(7)	5.4(4)
C(64)	0.641(1)	−0.114(1)	0.1554(7)	5.5(4)
C(65)	0.590(1)	−0.101(1)	0.1989(6)	5.1(4)
C(66)	0.530(1)	−0.0378(9)	0.2011(6)	4.3(4)
H(1)	0.276	0.078	0.022	4.0*
H(2)	0.315	0.179	0.121	4.0*
H(3)	0.286	0.034	0.124	4.0*

[a] See footnote *a* for Table 3.

nation site brought about by ligand motion over the face of the cluster. We suggest that the much faster rate of reaction of **2** with triphenylphosphine is a consequence of a more electron-rich Os(1) in **2** compared with **1**, which leads to a weak C=N–Os(1) interaction. This weaker interaction is manifest in the C(1)–Os(1) and N–Os(1) bond lengths, which are both 2.25(1) Å in **1** and 2.35(2) and 2.29(2) Å, respectively, in **2** and provides a larger pocket for attack of the phosphine in the Os(1)–C=N interaction. Previous stereochemical studies have shown that approach of the phosphine to **1** is distinctly a topside attack on the Os–C=N interaction.[10c]

The structural changes observed on going from **2** to **5** have significant consequences for the dynamic properties of the latter. Thus, the $^{31}P\{^1H\}$ NMR spectrum of **5** at −50 °C shows one major set of two resonances at −1.65 and −1.35 ppm relative to external H_3PO_4 (relative intensity ~2:1), a set of broadened resonances at −2.35 and −2.95 ppm (relative intensity ~2:1), and a set of sharp resonances at −6.31 and −6.90 ppm (relative intensity ~2:1) (Figure 3). The overall relative intensity of these sets of resonances is 7.2:1.4:1.0. In addition, there are two very minor resonances at +0.25 and 1.15 ppm. The resonance at +0.25 ppm shows a

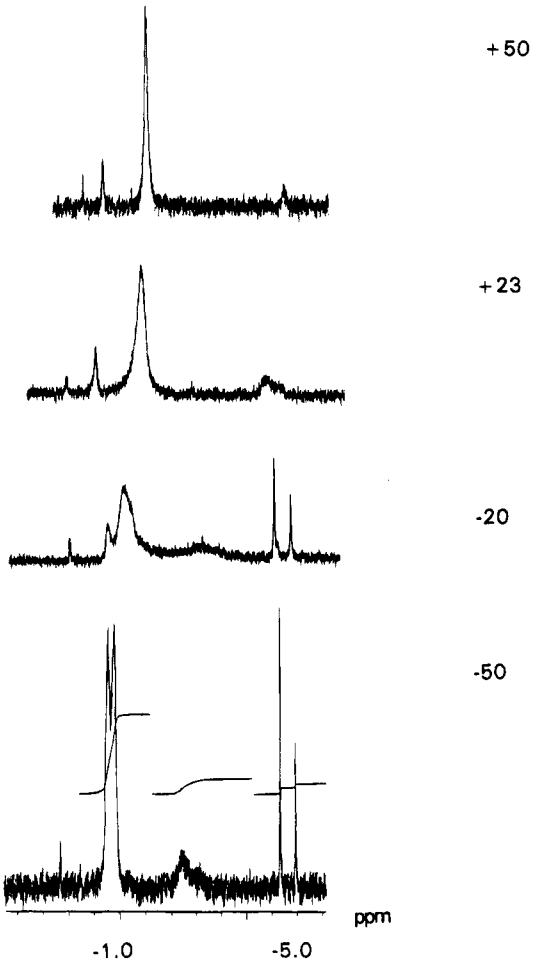

Figure 3. VT $^{31}P\{^1H\}$ NMR spectra of **5** at 161 MHz in $CDCl_3$.

significant chemical shift dependence and appears to have shifted under the major set of resonances at −50 °C. Neither of these resonances shows significant line broadening with decreasing temperature to −50 °C. At −80 °C in methylene chloride, we can observe the resonance at 0.25 ppm as a shoulder on the major resonance set but resolution of the latter is lost. The resonances at −2.95 and −2.35 ppm sharpen slightly at −80 °C.

The ^1H NMR of **5** at −50 °C consists of three sharp complex multiplets centered at −8.94, −15.74, and −17.97 ppm (relative intensity) 1:1.2:1.1). In addition, we observe a series of sharp multiplets ranging in relative intensity from 0.02:1 to 0.13:1 with respect to the major isomers at −8.18, −9.66, −12.76, −15.08, and −17.28 ppm. Furthermore, there are broad resonances at −8.01 and −15.90 ppm, each in a relative intensity of 0.14:1 with respect to the major resonances (Figure 4). As the temperature is increased to room temperature, we observe a broadening of the major resonances while the sets of sharp minor resonances remain sharp until +10 °C and the two initially broad resonances have merged with the base line. At room temperature we observe the averaging of the three sets of bridging hydride resonances and the onset of broadening of the resonances at −9.66 and −12.16 ppm, while the terminal hydride resonance due to the major isomer has merged into the base line. At +50 °C, a narrowing resonance appears at −16.75 ppm, the approximate average of the two bridging hydrides of the major

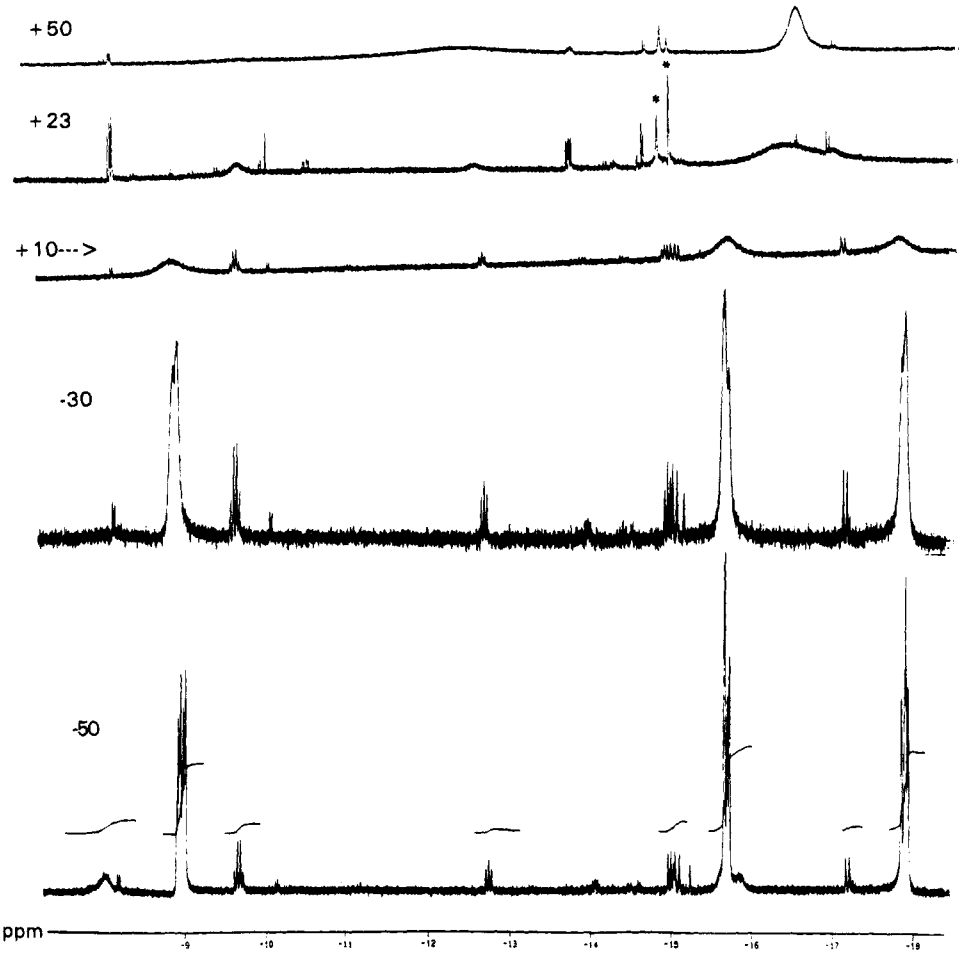

Figure 4. VT ^{1}H NMR spectra of **5** at 360 MHz (asterisks denote trace amounts of **3** and **6** present in the sample).

isomer. In the room-temperature spectrum a broad shoulder can be seen on the merging resonances at −17.20 ppm, which is the approximate average of the broad minor bridging hydride at −15.90 ppm (partially overlapping with the major bridging hydride resonance at −15.74 ppm) observed at −50 °C and a second bridging hydride which is apparently hidden under the major bridging hydride resonance at −17.97 ppm. This proposal is consistent with the fact that this bridging hydride resonance has an 11% higher integration than the terminal hydride resonance of the major isomer, which is well separated from its minor isomer counterparts. As for the ^{31}P{^{1}H} NMR data there appears a set of isomers which is more fluxional than the major isomer set (the broadened resonances in the −50 °C spectrum at −8.01, −15.90, and −17.97 ppm) and a set of minor isomers which is slightly more rigid than the major isomer set (the resonances at −9.66 and −15.08 ppm and a companion bridging hydride under the major resonance at −15.74 ppm; the latter is integrated about 20% higher than the terminal hydride). The lower intensity resonances remain rigid throughout the temperature range examined, except for the one at −12.76 ppm, which begins to broaden at ambient temperatures.

From the above ^{1}H NMR data, we cannot conclude whether the bridging and terminal hydrides are actually exchanging with each other. However, a 2D-EXSY experiment conducted at −50 °C with a mixing time of 0.5 s reveals that this is indeed the case. Furthermore, the complexity of the hydride multiplets observed for the major isomer does not clearly show that each resonance represents an isomer set of two. This is however, clearer from the phosphorus-decoupled ^{1}H NMR spectra at −50 °C (Figure 5), where each of the bridging hydride resonances appears as a partially overlapping set of doublets. Given that coupling between bridging hydrides is usually <1 Hz, the spectrum is clearly assignable to two isomers. As expected, the terminal hydride which is coupled to both μ-hydrides appears as a more complex multiplet (Figure 5).

There are in all 12 possible isomers for **5**. If one excludes the isomers with PPh_3 in the axial positions, this reduces to 6 (Scheme 1). The variable-temperature ^{1}H and ^{31}P NMR spectra show that there are three sets of isomers (which are present in comparable relative intensities for both nuclei) averaging at different rates. We suggest that these three sets differ by the location of the terminal hydride. We further propose that its position controls the rate of tripodal rotation at the osmium atom bearing the terminal hydride and that this process energetically overlaps with bridge−terminal hydride exchange. There are additional resonances which are extremely low in intensity that show up in the long-term accumulation at room temperature (Figure 4). These may be persistent trace impurities or other isomer sets. They will not be considered further. In our previous work on the dynamics of a range of imidoyl complexes of the type (μ-H)(μ-η^2-RC=NR′)$Os_3(CO)_9L$ (L = CO, PR_3), where L is located on the unbridged osmium atom analogously to **5**, we found that tripodal motion first involves three ligands only, excluding the axial ligand on the same face of the triangle as

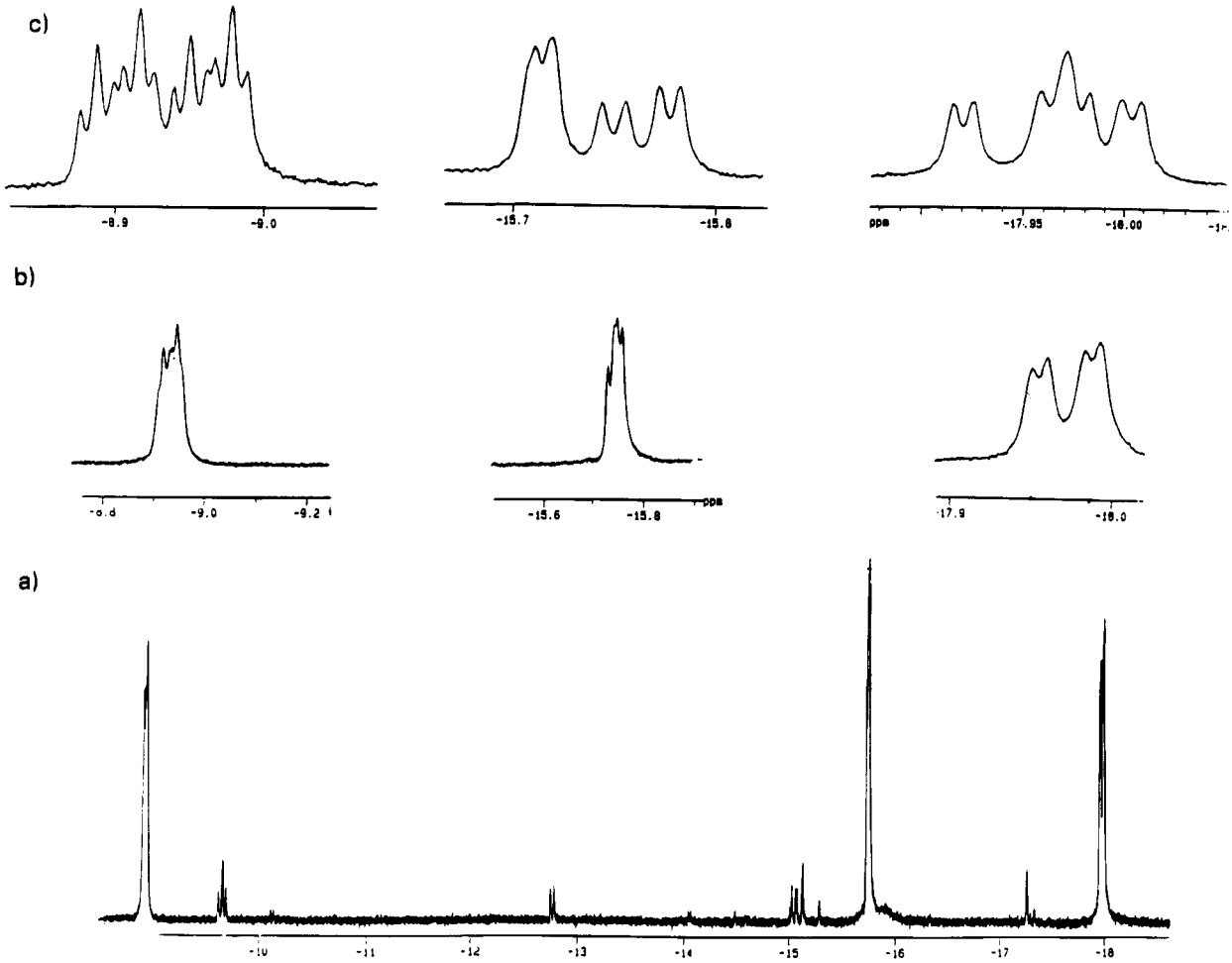

Figure 5. Phosphorus-decoupled ^{1}H NMR spectrum of **5**: (a) entire hydride region; (b) expansion of major isomer hydride resonances; (c) expansion of major isomer resonances with phosphorus coupling.

Scheme 1[a]

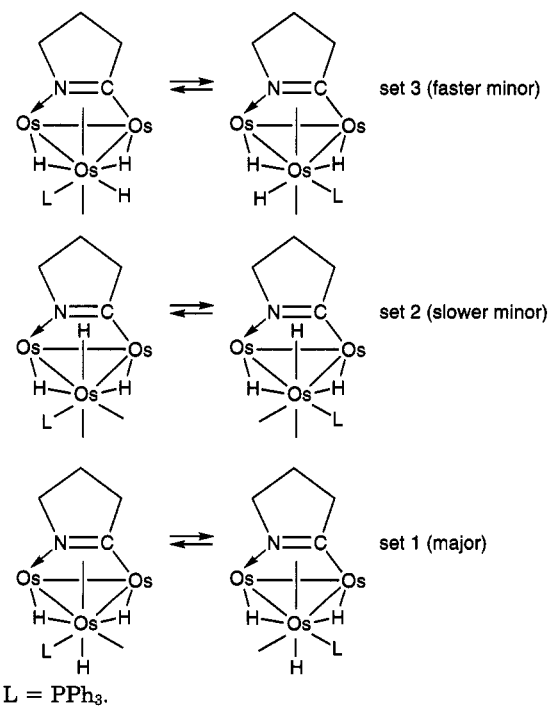

[a] L = PPh_3.

the imdoyl ligand.[10,11,13] On this basis we can assign the slowest set of exchanging hydrides to the minor isomer set 2 (Scheme 1). The major isomer set can be assigned to set 1 on the basis of the solid-state structure, where the terminal hydride is axial but is on the opposite face of the metal triangle to the imidoyl ligand. The rapidly exchanging isomer is probably set 3, where the hydride and the phosphine are both in radial positions. Of course, the assignment of the minor isomers must be taken as tentative, since there is no firm basis for excluding isomers with the phosphine in the axial position, but the more important aspect of these results is the much greater flexibility of **5** compared with **2**. We have previously observed that phosphine substitution leads to a lowering of the barrier to tripodal motion as in the unbridged osmium atom in $(\mu\text{-H})(\mu\text{-}\eta^2\text{-}\overline{C{=}NCH_2CH_2CH_2})Os_3(CO)_9L$ (L = CO, PR_3) complexes.[10] In **5**, however, this process apparently overlaps with bridge–terminal hydride exchange. This is probably a result of the elongation of the metal–metal bonds relative to those in **2** which would result in longer, weaker hydrogen–metal bridges. The greater mobility may be the result of significant asymmetry in the hydride bridges induced by phosphine substitution, but this is not evident, since our version of HYDEX places all bridging hydrides symmetrically. It is clear, however, that the proximity of the bridging and terminal hydrides is not related to their rate of exchange since they are much closer to each other in **2** than in **5**. Like **2**, **5** is thermally labile at elevated temperatures, undergoing nonspecific decomposition along with the formation of small amounts of **1**, **3**, and **6**.

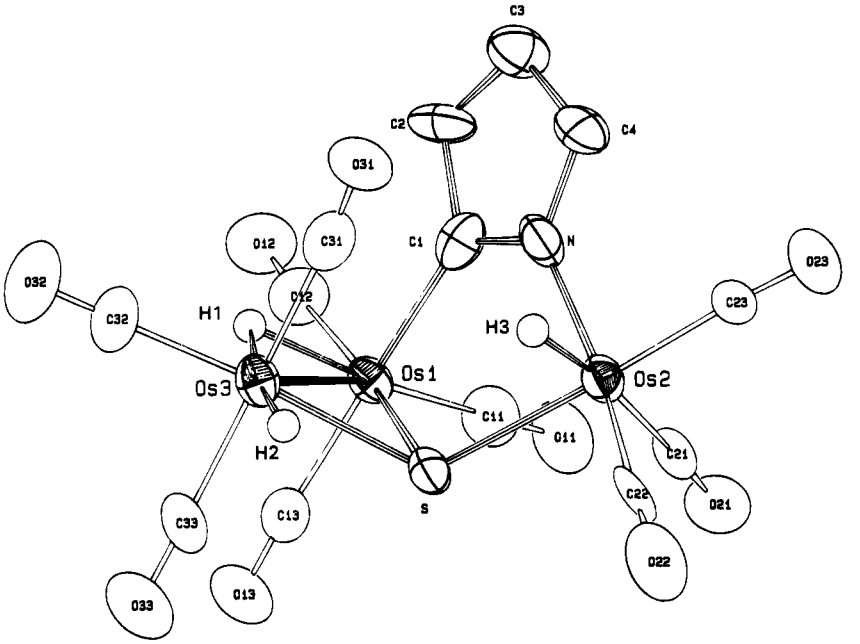

Figure 6. ORTEP drawing of $H_2(\mu\text{-}H)(\mu_3\text{-}S(\mu\text{-}\eta^2\text{-}C{=}NCH_2CH_2CH_2)Os_3(CO)_9$ (**7a**) showing the calculated positions of the hydrides.

Under an atmosphere of carbon monoxide in refluxing hexane **5** gives **6** in 60% yield (eq 3). Compound **6** is also obtained by addition of triphenylphosphine to **1** at room temperature.[13]

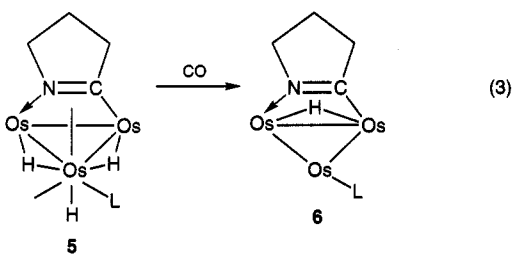

5 **6** (3)

The prevalence of sulfur-capped and sulfur-bridged clusters, particularly noted in the studies of Adams and co-workers,[14-17] demonstrates the unique properties of sulfur in the reactions of transition-metal clusters. In light of the fact that **1** is a reactive metal cluster and that H_2S reacts with $Os_3(CO)_{12}$,[18] $(\mu\text{-}H)_2Os_3(CO)_{10}$, and $(CH_3CN)_2Os_3(CO)_{10}$,[1b,14-17] we were interested to see if sulfur could be added to this cluster and what the structural consequences of H_2S addition would be compared with the observed direct addition of HCl.[19] The presence of an additional hydrogen could lead to further rearrangement of the cluster.

The reaction of **1** with gaseous hydrogen sulfide at room temperature in methylene chloride leads to quantitative conversion (by NMR) to two isomeric compounds whose formula, $H_2(\mu\text{-}H)(\mu_3\text{-}S)(\mu\text{-}\eta^2\text{-}C{=}NCH_2CH_2CH_2)Os_3(CO)_9$ (**7a,b**; isolated yields 44 and 22%, respectively), is based on ^1H NMR, infrared, and elemental analysis. The observation of two resonances in the terminal hydride region at −3.24 (s) and −10.11 (d, $^2J_{H-H}$ = 14.65 Hz) ppm as well as a bridging hydride at −14.54 (d, $^2J_{H-H}$ = 14.65 Hz) ppm led us immediately to attempt a solid-state structure determination of the major isomer. The structure is shown in Figure 6. Crystal data are given in Table 1, and selected bond distances and angles are given in Table 6 and atomic coordinates in Table 7. The structure consists of three osmium atoms with *only one* metal−metal bond (Os(1)−Os(3) = 2.993(1) Å). The other metal−metal distances are clearly too long for there to be any appreciable bonding interaction (Os(1)−Os(2) = 3.861 Å and

Table 6. Selected Bond Distances (Å) and Angles (deg) for 7a[a]

	Distances		
Os(1)−Os(3)	2.993(1)	N−C(1)	1.33(3)
Os(1)−S	2.423(6)	N−C(4)	1.45(2)
Os(2)−S	2.440(5)	C(1)−C(2)	1.54(3)
Os(3)−S	2.422(4)	C(2)−C(3)	1.53(4)
		C(3)−C(4)	1.47(4)
Os(2)−N	2.12(2)	C−O	1.14(3)
Os(1)−C(1)	2.09(2)		
Os−C(CO)	1.92(2)[b]	Os(1)−H(1)	1.85[c]
		Os(2)−H(3)	1.61[c]
		Os(3)−H(1)	1.85[c]
		Os(3)−H(2)	1.61[c]
	Angles		
Os(3)−Os(1)−S	51.8(1)	C(1)−Os(1)−S	86.9(7)
Os(1)−Os(3)−S	51.9(1)	N−Os(2)−S	85.7(4)
Os(1)−S−Os(3)	76.3(2)		
Os(1)−S−Os(2)	105.1(2)	H1−Os(3)−H(2)	171[c]
		Os(1)−H1−Os(3)	108[c]
Os−C−O	175.7(2)	S−Os(2)−H(3)	84[c]

[a] Numbers in parentheses are estimated standard deviations. [b] Average values. [c] Values calculated using HYDEX.[12]

(14) Adams, R. D.; Babin, J. E.; Mathur, P.; Natarajan, K.; Wang, J. *Inorg. Chem.* **1989**, *28*, 1440 and references therein.
(15) Adams, R. D.; Babin, J. E.; Tasi, M. *Inorg. Chem.* **1988**, *27*, 2618 and references therein.
(16) Adams, R. D.; Tanner, J. T.; Chen, G.; Yin, J. *Organometallics* **1990**, *9*, 595.
(17) Adams, R. D.; Babin, J. E.; Wang, J.; Wu, W. *Inorg. Chem.* **1989**, *28*, 703.
(18) Deeming, A. J.; Underhill, M. *J. Organomet. Chem.* **1972**, *42*, C60.
(19) (a) Gobetto, R.; Hardcastle, K. I.; Kabir, S. E.; Milone, L.; Nichimura, N.; Osella, D.; Rosenberg, E.; Yin, M. *J. Am. Chem. Soc.*, submitted for publication. (b) Hardcastle, K. I.; Irving, M. *J. Cluster Sci.* **1993**, *4*, 77.

Table 7. Fractional Atomic Coordinates for 7a

atom	*x*	*y*	*z*	*B* (Å²)[a]
Os(1)	0.30451(7)	−0.21820(6)	0.33989(6)	2.48(1)
Os(2)	0.56199(7)	−0.37941(6)	0.24288(6)	2.64(1)
Os(3)	0.28194(7)	−0.38169(6)	0.47488(6)	2.69(2)
S	0.3374(4)	−0.3700(4)	0.2852(4)	2.8(1)
O(11)	0.371(2)	−0.122(1)	0.131(1)	4.8(4)
O(12)	0.261(2)	−0.044(1)	0.456(1)	5.6(4)
O(13)	0.022(1)	−0.241(1)	0.269(1)	5.0(4)
O(21)	0.502(2)	−0.276(1)	0.031(1)	5.0(4)
O(22)	0.520(2)	−0.553(2)	0.130(1)	6.6(5)
O(23)	0.844(1)	−0.400(2)	0.199(1)	6.0(5)
O(31)	0.554(1)	−0.382(1)	0.573(1)	4.4(4)
O(32)	0.190(2)	−0.391(2)	0.706(1)	6.5(5)
O(33)	0.011(2)	−0.430(1)	0.399(1)	5.6(4)
N	0.586(1)	−0.271(1)	0.351(1)	3.5(4)
C(1)	0.497(2)	−0.216(2)	0.385(1)	3.3(4)
C(2)	0.557(2)	−0.148(2)	0.464(2)	4.0(5)
C(3)	0.694(2)	−0.180(2)	0.479(2)	3.9(5)
C(4)	0.709(2)	−0.255(2)	0.404(2)	4.3(5)
C(11)	0.346(2)	−0.159(2)	0.209(2)	3.5(4)
C(12)	0.273(2)	−0.109(2)	0.413(2)	3.5(5)
C(13)	0.122(2)	−0.230(2)	0.296(1)	3.6(5)
C(21)	0.526(2)	−0.311(1)	0.112(2)	2.7(4)
C(22)	0.531(2)	−0.482(2)	0.170(2)	3.5(5)
C(23)	0.740(2)	−0.391(2)	0.217(1)	4.0(5)
C(31)	0.460(2)	−0.379(2)	0.533(1)	3.7(5)
C(32)	0.220(2)	−0.384(2)	0.619(2)	5.5(7)
C(33)	0.112(2)	−0.413(2)	0.426(2)	3.3(4)
H(1)	0.271	−0.260	0.478	4.0*
H(2)	0.308	−0.486	0.461	4.0*
H(3)	0.573	−0.441	0.349	4.0*

[a] See footnote *a* for Table 3.

Os(2)–Os(3) = 4.151 Å). The imidoyl ligand bridges the shorter of the two nonbonded edges and donates three electrons to the cluster *via* a two-electron-donor σ-bond between nitrogen and Os(2) and a one-electron σ-bond from C(1) to Os(1) (N–Os(2) = 2.12(2) Å and C(1)–Os(1) = 2.09(2) Å). The sulfur atom bridges all three osmium atoms and donates four electrons overall to the metals through three nearly equivalent bonds to osmium (S–Os(1) = 2.42(1) Å, S–Os(2) = 2.44(1) Å, and S–Os(3) = 2.42(1) Å). One hydride (located using HYDEX[12]) was found to bridge the metal–metal bond and to lie 0.90 Å above the three-metal-atom plane and is *trans* to CO(11) and one of the terminal hydride ligands (H(1)–Os(3)–H(2) = 171.1°). The other terminal hydride ligand was located on Os(2) *trans* to CO(21). This bonding arrangement makes **7a** a 52-valence-electron saturated cluster. The exceptionally large H–H coupling observed in **7a** (14.65 Hz) is the largest such coupling observed in an osmium cluster and is undoubtedly a consequence of the direct *trans* relationship between the bridging and terminal hydrides.[2a,4] On the basis of the X-ray crystallographic data for **7a** and the similarity of the ^{1}H NMR spectra of **7a** and **7b**, we can assign a structure for **7b** as an exact analog of **7a** in which C(1) and N have exchanged positions. Another alternative structure is one where the terminal hydrides are *anti* to each other as opposed to the *syn* orientation observed in **7a** (Scheme 2). The first alternative is supported by the differences in the chemical shifts for the hydrides. The bridging hydride in **7a** has a chemical shift of −14.85 ppm, whereas **7b** shows a chemical shift of −12.95 ppm. Additionally, the terminal uncoupled hydride has a chemical shift of −3.24 ppm in **7a** and −4.52 ppm in **7b**, while there is very little difference in the chemical shifts of the coupled terminal hydride, −10.20 ppm in **7a** and −9.85 ppm in **7b**. The formation of isomers differing by the disposition of the imidoyl bridge in **7a** and **7b** is further supported by the expected pathway of formation if the first sulfur–hydrogen bond addition follows the same pathway as that observed for HX (X = Cl, Br, CF_3CO_2);[19] the initial two isomers formed could then react with the second sulfur–hydrogen bond at one of two available metal edges (Scheme 2). It has been a general observation of ours that the solid-state structures of the products formed from the reaction of μ_3-imidoyl clusters with electron donors are indeed kinetically determined as proposed here.[10,11,13,19]

Scheme 2

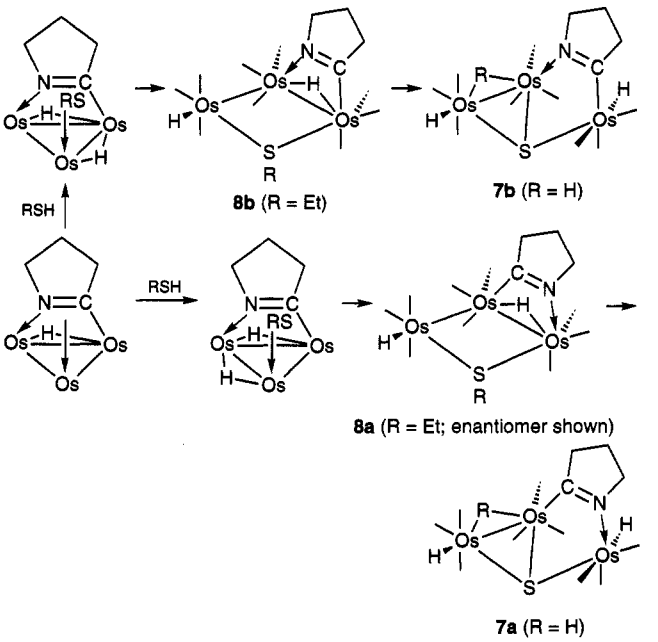

The reaction of **1** with ethanethiol lends further support to the above proposed reaction pathways. A methylene chloride solution of **1** was reacted with 10-fold excess of ethanethiol at room temperature for 24 h. A single product band was isolated in 67% yield. The ^{1}H NMR and infrared spectra and elemental analysis are consistent with the formula H(μ-H)(μ-SCH_2CH_3)(μ-η^2-C(=$NCH_2CH_2CH_2$)$Os_3(CO)_9$ (**8**). As for **7**, the hydride region of the ^{1}H NMR spectrum indicates the presence of two isomers in solution of approximately equal intensity, giving four hydride resonances at −9.88 (s), −10.17 (s), −12.30 (s), and −12.72 (s) ppm. Since no coupling is observed between the terminal and bridging hydride resonances (even in COSY and TOCSY experiments), we propose a structure where one metal–metal bond has cleaved and where the bridging hydride still bridges the imidoyl-bridged edge of the triangle (eq 4).

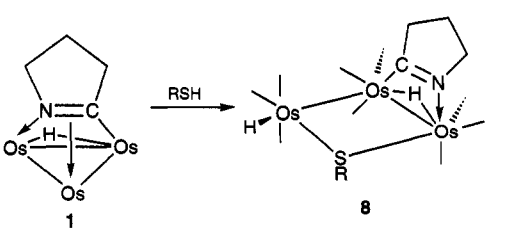

(4)

Here as for **7** we propose that the two isomers differ in the disposition of the imidoyl ligand and that the reaction pathway is directly analogous to that of **1** with H_2S. The reaction was conducted using ethanethiol-*d*

and followed by ^1H NMR. We observed equal proton populations present in both bridging and terminal hydride positions, indicating that randomization of hydrides is faster than metal–metal bond cleavage (Scheme 2).

Although **7** is quite different than the other trihydride clusters reported here, there are two examples of sulfur-bridged triosmium clusters containing one metal–metal bond, namely $(\mu_3\text{-S})(\mu\text{-CH}_2\text{S})(\text{PPhMe}_2)\text{Os}_3(\text{CO})_9$ and $(\mu\text{-H})(\mu_3\text{-S})(\mu\text{-CH}_2\text{S})(\text{PPhMe}_2)\text{Os}_3(\text{CO})_8\text{Cl}$.[20,21] Here as in the case of **7** the cluster is primarily supported by a μ_3-S group and contains a bridging organic ligand. Compound **7** differs in being a relatively hydrogen rich cluster. The further reaction chemistry of **2**, **5**, **7**, and **8** is currently under investigation.

Experimental Section

Unless otherwise stated, purification of solvents and reactions were carried out under an atmosphere of nitrogen. Hexane and THF were distilled from sodium benzophenone ketyl and methylene chloride from calcium hydride prior to use. Octane was stored over sodium wire and purged with nitrogen prior to use. Hydrogen sulfide was purchased from Matheson and used as received. Triphenylphosphine and ethanethiol were purchased from Aldrich and used without further purification. The cluster $(\mu\text{-H})(\mu_3\text{-}\eta^2\text{-}\overline{\text{C=NCH}_2\text{CH}_2\text{CH}_2})\text{Os}_3(\text{CO})_9$ was prepared as described previously.[10] IR spectra were recorded on a Perkin-Elmer 1420 spectrophotometer. ^1H NMR spectra were obtained on a Bruker AMX 360 or Varian Unity Plus 400 or IBM NR-80 spectrometer. Elemental analyses were performed by Schwarzkopf Microanalytical Laboratory (New York). Photochemical reactions were carried out using a Rayonet photochemical reactor irradiating with 3000 Å lamps.

Reaction of $(\mu\text{-H})(\mu_3\text{-}\eta^2\text{-}\overline{\text{C=NCH}_2\text{CH}_2\text{CH}_2})\text{Os}_3(\text{CO})_9$ (1) with H_2. (a) Thermal Route. Hydrogen gas was bubbled through a refluxing octane solution (100 mL) of **1** (0.080 g, 0.090 mmol) for 9 h. The solvent was then rotary evaporated. The residue was dissolved in a minimum volume of CH_2Cl_2 and chromatographed by TLC on silica gel. Elution with hexane/CH_2Cl_2 (10:3 v/v) gave four bands. The first yellow band gave the known compound $(\mu\text{-H})_2(\mu\text{-}\eta^2\text{-}\overline{\text{C=NCH}_2\text{CH}_2\text{CH}_2})_2\text{Os}_3(\text{CO})_8$[11] (**4**) (0.004 g, 10% based on consumed **1**). The second band gave $(\mu\text{-H})(\mu\text{-}\eta^2\text{-}\overline{\text{C=NCH}_2\text{CH}_2\text{CH}_2})\text{Os}_3(\text{CO})_{10}$[10a] (**3**) (0.010 g, 24% based on consumed **1**). The third band gave unconsumed **1** (0.040 g); the fourth band yielded $\text{H}(\mu\text{-H})_2(\mu_3\text{-}\eta^2\text{-}\overline{\text{C=NCH}_2\text{CH}_2\text{CH}_2})\text{Os}_3(\text{CO})_8$ (**2**) (0.039 g, 46% based on consumed **1**) as pale yellow crystals from CH_2Cl_2/hexane at −20 °C.

Spectral and Analytical Data for 2. IR (ν(CO) in hexane): 2088 w, 2063 vw, 2051 s, 2041 s, 2013 s, 1991 m, 1982 w cm^{-1}. ^1H NMR (400 MHz; in $CDCl_3$): 3.61 (m, 1 H), 3.45 (m, 1H), 3.17 (dd, 1H), 2.14 (m, 1H), 2.02 (m, 1H), 1.66 (m, 1H), −9.65 (s, 1H), −15.31 (d, J_{H-H} = 2.4 Hz, 1H), −15.89 (d, J_{H-H} = 2.4 Hz, 1H) ppm. ^{13}C NMR ($CDCl_3$): 177.56 (d, J_{C-H} < 2 Hz), 177.17 (d, J_{C-H} < 2 Hz), 175.55 (d, J_{C-H} = 12 Hz), 174.80 (J_{C-H} = 9 Hz), 170.92 (m), 169.23 (m), 168.57 (d, J_{C-H} < 2 Hz), 166.24 (d, J_{C-H} < 2 Hz). Anal. Calcd for $C_{12}H_9NO_8Os_3$: C, 16.65; H, 1.05; N, 1.62. Found: C, 16.94; H, 1.05; N, 1.40.

(b) Photochemical Route. A solution of compound **1** (0.101 g, 0.113 mmol) in hexane (100 mL) in a 200-mL quartz flask was irradiated for 1 h while hydrogen was bubbled through it. The solvent was removed *in vacuo*, and chromatographic separation of the residue as described above gave four bands. The fastest and slowest moving bands each gave a small quantity (~0.003 g) of an uncharacterized compound. The second band afforded unreacted **1** (0.040 g). The third band gave **2** (0.028 g, 47% based on consumed **1**).

Reaction of 2 with PPh_3. To a hexane solution of **2** (0.045 g, 0.052 mmol) was added PPh_3 (0.027 g, 0.104 mmol), and the reaction mixture was stirred at room temperature for 24 h. Analytical TLC showed total consumption of **2**. The color changed from pale yellow to orange. The solvent was removed under vacuum, and the residue was chromatographed by TLC on silica gel. Elution with hexane/CH_2Cl_2 (10:2, v/v) gave two bands. The fastest moving band gave a small quantity (~0.002 g) of an uncharacterized compound, while the second band yielded $\text{H}(\mu\text{-H})_2(\mu\text{-}\eta^2\text{-}\overline{\text{C=NCH}_2\text{CH}_2\text{CH}_2})\text{Os}_3(\text{CO})_8\text{PPh}_3$ (**5**) as yellow crystals from hexane/CH_2Cl_2 at −20 °C (0.050 g, 86%).

Spectral and Analytical Data for 5. IR (ν(CO) in hexane): 2079 m, 2043 s, 2023 w, 2005 m, 1996 sh, 1980 w, 1963 w cm^{-1}. ^1H NMR (360 MHz; (in $CDCl_3$ at −50 °C, low-temperature limit): major isomer 3.53 (m, 1H), 2.49 (m, 1H), 2.29 (m, 1H), 2.25 (m, 1H), 1.64 (m, 2H), −8.94 (m, J_{P-H} = 10.5 and 10 Hz, J_{H-H} = 3 and 4 Hz, 1H), −15.74 (m, J_{P-H} = 9 and 12.5 Hz, J_{H-H} = 3 and 4 Hz, 1H), −17.97 (m, J_{P-H} = 18 and 14.4 Hz, J_{H-H} = 3 and 4 Hz, 1H) ppm. Anal. Cacld for $C_{30}H_{24}NO_8POs_3$: C, 31.93; H, 2.15; N, 1.24. Found: C, 32.09; H, 1.98; N, 1.21.

Kinetics of the Reaction of 2 with PPh_3. Samples of **2** (0.028 g, (0.041 mmol) and 0.017 g (0.028 mmol)) were each dissolved in 0.7 mL of $CDCl_3$ in 5 mm NMR tubes. Triphenylphosphine (0.012 g, (0.045 mmol) and 0.008 g (0.031 mmol)) was added as a solid to the NMR tubes. The tubes were shaken and then immediately inserted into the NMR probe thermostated at +23 °C. An ^1H NMR spectrum of the hydride region (−8 to −17 ppm) of **2** was taken within 2 min of addition, and then one was taken every 1 h in the first run and every 20 min in the second run. A resonance at −8.9 ppm due to the formation of a mononuclear hydride complex was noted, but its intensity did not change over the course of the run and is assumed to be due to some initial fragmentation of **2** in the presence of high local concentrations of PPh_3. The peak areas of the hydrides of **2** were compared to those in the first spectrum, and concentrations were determined. The first six points were fit to the integrated second-order equation for equal reactant starting concentrations ($1/A = 1/A_0 + kt$) to give an average value for the two runs of 2.0 ± 1.2 M^{-1} min^{-1}. Second-order kinetics was assumed on the basis of the known second-order behavior of **1** reacting with phosphines.[10c] The calculated half-life for this reaction is 12.5 min; therefore, the <2 min; before the first spectrum is taken is significant, accounting for the large reported error.

Reaction of 5 with CO. Carbon monoxide gas was bubbled through a refluxing hexane solution (25 mL) of **5** (0.010 g) for 2 h. The solvent was removed *in vacuo*, and the residue was chromatographed by TLC on silical gel. Elution with a hexane/CH_2Cl_2 (10:3 v/v) mixture gave one main band, which yielded $(\mu\text{-H})(\mu\text{-}\eta^2\text{-}\overline{\text{C=NCH}_2\text{CH}_2\text{CH}_2})\text{Os}_3(\text{CO})_9\text{PPh}_3$ (**6**; 0.060 g, 60%).

Reaction of 1 with H_2S. Hydrogen sulfide gas was bubbled through a dichloromethane solution (15 mL) of **1** (0.052 g, 0.058 mmol) for 4 min, and the reaction mixture was stirred for an additional 10 min. The solvent was removed *in vacuo*, and the residue was chromatographed by TLC on silica gel. Elution with a hexane/CH_2Cl_2 (10:2 v/v) mixture resolved four bands. The fastest moving, colorless band gave $\text{H}_2(\mu\text{-H})(\mu_3\text{-S})\mu\text{-}\eta^2\text{-}\overline{\text{C=NCH}_2\text{CH}_2\text{CH}_2})\text{Os}_3(\text{CO})_9$ (**7a**; 0.024 g, 44%) as pale yellow crystals after recrystallization from hexane/CH_2Cl_2 at −20 °C. The second band gave **7b** (0.012 g, 22%) as

(20) Adams, R. D.; Golembeski, N. M.; Selegue, J. P. *J. Am. Chem. Soc.* **1979**, *101*, 5862; **1981**, *103*, 546.
(21) Adams, R. D.; Golembeski, N. M.; Selegue, J. P. *Organometallics* **1982**, *1*, 240.

pale yellow crystals. The third and the fourth bands each gave too small an amount for further characterization.

Spectral and Analytical Data for 7a. IR (ν(CO) in hexane): 2112 w, 2094 s, 2083 s, 2074 w, 2042 s, 2028 vs, 2010 vs, 2004 vs, 1999 vs cm^{-1}. ^{1}H NMR (80 MHz; in $CDCl_3$): 4.04 (m, 2H), 3.00 (m, 2H), 1.72 (m, 2H), −3.24 (s, 1H), −10.11 (d, $^2J_{H-H}$ = 14.65 Hz, 1H), −14.5 (d, $^2J_{H-H}$ = 14.65 Hz, 1H) ppm. Anal. Calcd for $C_{13}H_9NO_9Os_3S$: C, 16.86; H, 0.98; N, 1.51. Found: C, 16.95; H, 1.02; N, 1.52.

Spectral and Analytical Data for 7b. IR (ν(CO) in hexane): 2114 w, 2094 s, 2086 s, 2082 vs, 2039 s, 2029 vs, 2016 vs, 2009 vs, 1997 vs cm^{-1}. ^{1}H NMR (400 MHz; in $CDCl_3$): 3.98 (m, 1H), 3.94 (m, 1H), 3.06 (m, 1H), 2.95 (m, 1H), 1.74 (m, 1H), 1.63 (m, 1H), −4.52 (s, 1H), −9.85 (d, $^2J_{H-H}$ = 14.16 Hz, 1H), −12.95 (d, $^2J_{H-H}$ = 14.16 Hz, 1H) ppm. Anal. Calcd for $C_{13}H_9NO_9Os_3S$: C, 16.86; H, 0.98; N, 1.51. Found: C, 16.98; H, 1.08; N, 1.49.

Reaction of 1 with CH_3CH_2SH. To a dichloromethane solution (15 mL) of **1** (0.100 g, 0.112 mmol) was added dropwise a dichloromethane solution (10 mL) of ethanethiol (0.120 g, 1.12 mmol) over a period of 30 min. The mixture was then stirred at room temperature for an additional 15 h. The volatiles were removed by blowing nitrogen through the solution. The residue was chromatographed by TLC on silica gel. Elution with hexane/CH_2Cl_2 (10:3 v/v) gave one main band, which yielded $H(\mu\text{-}H)(\mu\text{-}SCH_2CH_3)(\mu\text{-}\eta^2\text{-}C(=NCH_2CH_2CH_2)\text{-}Os_3(CO)_9$ (**8**; 0.068 g, 64%) as yellow crystals.

Spectral and Analytical Data for 8. IR (ν(CO) in hexane): 2102 w, 2085 s, 2073 w, 2060 w, 2043 s, 2030 s, 2023 vs, 2016 s, 2009 vs, 1999 s, 1997 s, 1971 w cm^{-1}. ^{1} NMR (80 MHz; in $CDCl_3$): 3.90 (m, 2H), 3.30 (m, 2H), 2.65 (m, 4H), 1.43 (m, 3H), −9.88 (s, 1H), −10.17 (s, 1H), −12.30 (s, 1H), −12.72 (s, 1H) ppm. Anal. Calcd for $C_{15}H_{13}NO_9Os_3S$: C, 18.88; H, 1.38; N, 1.47. Found: C, 19.35; H, 1.65; N, 1.55.

Deuterium-Labeling Experiment for the Reaction of EtSD with 1. To EtSD (21 μL in 0.7 mL of $CDCl_3$, 0.42 mmol, prepared by exchange of EtSH with D_2O and checked by ^{1}H NMR) was added 0.020 g (0.022 mmol) of **1**. The ^{1}H NMR showed complete reaction after 10 min, and the distribution of protons in the hydrides did not change with time.

X-ray Structure Determination of 2, 5, and 7a. Crystals of **2**, **5**, and **7a** for X-ray examination were obtained from saturated solutions of each in hexane/dichloromethane solvent systems at −20 °C. Suitable crystals of each were mounted on glass fibers, placed in a goniometer head on the Enraf-Nonius CAD4 diffractometer, and centered optically. Unitl cell parameters and an orientation matrix for data collection were obtained by using the centering program in the CAD4 system. Details of the crystal data are given in Table 1. For each crystal, the actual scan range was calculated by scan width = scan range + 0.35 tan θ and backgrounds were measured by using the moving-crystal–moving-counter technique at the beginning and end of each scan. Two or three representative reflections were monitored every 2 h as a check on instrument and crystal stability, and an additional two reflections were monitored for crystal orientation control. Lorentz, polarization, and decay corrections were applied, as was an empirical absorption correction based on a series of ψ scans for **2** and **7a**. No absorption correction was made for **5**. The weighting scheme used is $1/\sigma^2$ based on counting statistics.

Each of the structures was solved by the Patterson method using SHELXS-86,[22] which revealed the positions of the metal atoms. All other non-hydrogen atoms were found by successive difference Fourier syntheses. The expected hydride positions were calculated by using the program HYDEX;[12] all other hydrogens were positioned using the program HYDRO.[23] Hydrogen atom positions were included in the structure factor calculations but not refined, in the final least-squares cycles. All non-hydrogen atoms were refined anisotropically.

The rather subtle difference in the otherwise symmetrical pyrrolidine ring (N *vs* C, seven electrons *vs* six) resulted in positional isomerism or disorder in the metal cluster **5**. This was taken into account by treating the Cl and N atoms of the ring as having an average electron density of 6.5, and these atoms are referred to as DN1 and DN2 in the tables. Final refinement parameters for each crystal are listed in Table 1.

Scattering factors were taken from Cromer and Waber.[24] Anomalous dispersion corrections were those of Cromer.[25] All calculations were carried out on a DEC MicroVAX II computer using the MOLEN system of programs.

All structures are illustrated using ORTEP–II, a FORTRAN thermal ellipsoid plot program for crystal structure illustrations.[26]

Acknowledgment. We gratefully acknowledge the National Science Foundation (Grant No. CHE9016495) for support of this research and for a Chemical Instrumentation Grant (Grant No. CHE8913125) for purchase of a 360-MHz NMR.

Supplementary Material Available: Tables 8–10, listing anisotropic displacement factors, and Tables 11–13, listing complete bond distances and angles, for **2**, **5**, and **7a** and Figure 7, giving the ^{13}C NMR of **2** including partial assignments, Figure 8, showing the kinetic stack plot of the conversion of **2** and **5** followed by ^{1}H NMR, and Figure 9, giving the 2D ^{1}H EXSY spectrum of **5** (22 pages). Ordering information is given on any current masthead page.

OM940422F

(22) Sheldrick, G. M. Program for Crystal Structure Solution; University of Gottingen, Gottingen, Germany, 1986.

(23) Schenk, H., Ollthof-Hazelkamp, R., von Konigsveld, H., Bassi, G. C., Ed.; *Computing in Crystallography*; Delft University Press: Delft, Holland, 1978; pp 64–74.

(24) Cromer, D. T.; Waber, J. T. *International Tables for X-ray Crystallography*; Kynoch Press: Birmingham, England, 1974; Vol. IV, Table 2.2B.

(25) Cromer, D. T. *International Tables for X-ray Crystallography*; Kynoch Press, Birmingham, England, 1974; Vol. IV, Table 2.3.1.

(26) Johnson, C. K. Report ORNL-3794, 3rd Revision; Oak Ridge National Laboratory: Oak Ridge, TN, 1976.